Journal of Alloys and Compounds 511 (2012) L1–L5

Contents lists available at SciVerse ScienceDirect

Journal of Alloys and Compounds

journal homepage: www.elsevier.com/locate/jallcom

Letter

Synthesis and characterization of multipod zinc oxide whiskers synthesized via a modified self-propagating high-temperature synthesis method

Cheng-Hsiung Peng[a], Ching-Chih Chang[b], Chyi-Ching Hwang[c,*]

[a] Department of Chemical and Materials Engineering, Minghsin University of Science and Technology, Xinfeng Township, Hsinchu County 304, Taiwan, ROC
[b] Chemical Systems Research Division, Chung Shan Institute of Science & Technology, Lungtan 325, Taiwan, ROC
[c] Department of Chemical and Materials Engineering, Chung Cheng Institute of Technology, NDU, Dasi, Taoyuan 335, Taiwan, ROC

ARTICLE INFO

Article history:
Received 31 July 2011
Received in revised form 9 September 2011
Accepted 13 September 2011
Available online 19 September 2011

Keywords:
SHS
ZnO whisker
Oxygen pressure
Photoluminescence
Microwave absorption

ABSTRACT

A self-propagating high-temperature synthesis (SHS) method, which features a 2-step heating process carried out in a closed chamber, was developed to prepare multipod ZnO whiskers (mZnOw). A compacted Zn powder was first heated at 370 °C in air to form a refractory layer of ZnO on the surface of Zn particles. Next, the SHS reaction was ignited by rapidly heating to ~750 °C under different oxygen gauge pressures (P_{O_2}) to obtain a loose white product mainly composed of mZnOw. It was found that the P_{O_2} strongly affected the reaction conversion and morphological features, along with the Zn-to-O ratio, of the as-synthesized products, which, in turn, might influence their photoluminescence and microwave absorption properties. A possible explanation for the effects of P_{O_2} on these characteristics was also proposed.

© 2011 Elsevier B.V. All rights reserved.

1. Introduction

Zinc oxide (ZnO) is an n-type semiconductor characterized by a direct band gap of 3.37 eV, a large exciton binding energy of 60 meV at room temperature, transparent conductivity, noncentrosymmetrical symmetry, and bio-safety and bio-compatibility properties [1–3]. Therefore, ZnO with different morphologies (e.g., particles, rods/fibers/wires, thin films) has recently attracted substantial attention from multiple researchers [3–7]. For example, multipod ZnO whiskers (mZnOw), which possess a peculiar shape and a single-crystalline character, have been cited for its potential use in optoelectronic and microwave-absorbing applications [3,8–10].

Two major categories of techniques have been developed for the synthesis of mZnOw, namely, thermal evaporation processes [11–13] and combustion methods [8,14] in which zinc powders are placed into either a pre-heated vacuum chamber or an open tube furnace and kept at elevated temperatures (600–1300 °C). The Zn powders undergo a sequence of changes including melting, evaporation, oxidation, and even combustion; consequently, the mZnOw can condense from the gas phase via nucleation and crystal growth. Both of these routes, however, may have implicit drawbacks, such as poor production efficiency, higher energy consumption, and the required addition of a catalyst (C or Au) [13]. Furthermore, extra equipment is necessary for the thermal evaporation processes to guarantee a suitable vacuum level and atmospheric control, giving rise to an increase in production cost. As for the combustion methods, a certain amount of both the Zn vapor and the as-synthesized mZnOw may be lost because the reaction is carried out with the furnace open to the air, thereby causing both a safety problem and difficulty in collecting the product.

In our previous study [15], a self-propagating high-temperature synthesis (SHS) method was developed for the synthesis of mZnOw. The combustion of the reactants (compacted Zn powder and NH_4NO_3 (5–15%)) was performed in a closed chamber under atmospheric pressure and little energy was required. Upon ignition, extra energy was no longer required because the combustion reaction was self-sustaining. Several problems, such as the process economy, safety, and product collection, which were encountered in the two routes mentioned above, can be partially minimized. Although the NH_4NO_3 additive was found to be essential for enhancing the product yield, its use causes the procedure to be somewhat more complicated and expensive. In addition, the pollutants $NH_{3(g)}$ and $NO_{x(g)}$ may be produced during the SHS reaction.

In this work, the SHS method was modified for the synthesis of mZnOw via a 2-step heating approach that omits the addition of NH_4NO_3. The developmental details of this process are described below. Moreover, the effects of oxygen gauge pressure (P_{O_2}) on the reaction conversion and the properties of the

* Corresponding author. Tel.: +886 3 3891716x114; fax: +886 3 3892494.
E-mail address: chyichinghwang@gmail.com (C.-C. Hwang).

0925-8388/$ – see front matter © 2011 Elsevier B.V. All rights reserved.
doi:10.1016/j.jallcom.2011.09.033

as-synthesized products (morphology, elementary composition ratio of Zn-to-O, photoluminescence (PL) properties, microwave-absorbing efficiency) were investigated and discussed.

2. Experimental procedures

2.1. Development of the SHS process

The reaction for ZnO formation, $Zn_{(s)} + (1/2)O_{2(g)} \rightarrow ZnO_{(s)}$, should be a strongly exothermic reaction according to the following calculation:

$$\frac{-(\Delta H_f^\circ)_{ZnO}}{(c_p)_{ZnO}} = \frac{348\ \text{kJ mol}^{-1}}{40.25 \times 10^{-2}\ \text{kJ mol}^{-1}\ \text{K}^{-1}} \approx 8.65 \times 10^3\ \text{K}$$

where $(\Delta H_f^\circ)_{ZnO}$ and $(c_p)_{ZnO}$ are the enthalpy of formation and the heat capacity of ZnO at the standard state (i.e., 298 K, 1 atm), respectively. This formula indicates that the reaction temperature of ZnO formation would exceed 8500 K under an adiabatic condition. Moreover, empirical observation suggests that reactions with a ratio of $-(\Delta H_f^\circ)_{ZnO}/(c_p)_{ZnO} \geq 2.0 \times 10^3$ K will, once ignited, lead to self-sustaining combustion fronts without requiring additional energy from an exterior heat source [16]. In practice, the melting and coalescence of $Zn_{(s,l)}$ can take place during the combustion reaction, due to the low melting point of Zn (419 °C), which eliminates the original pores of the compacted Zn powders and thereby inhibits the penetration/diffusion of oxygen from the outside. Although the combustion reaction can be ignited, it soon ceases.

Our previous study [15] confirmed that by adding NH_4NO_3 to the compacted Zn, the oxidizing species, NO_x and O_2, which are generated from the decomposition of NH_4NO_3 during the early heating stage, can react with Zn to form ZnO_{1-x}. This layer of zinc oxide would protect the underlying zinc, as the Pilling-Bedworth ratio is 1.61; this ratio indicates that the ZnO film is nonporous and adherent to the Zn particle [17]. Consequently, the ZnO layer can act as a refractory skin because its melting point (1975 °C) is higher than that of Zn, which allows it to cover the surface of the Zn and prevent the compacted Zn powder from collapsing during the SHS reaction. Next, oxygen could continuously penetrate into the compacted powder, resulting in the complete combustion and a higher reaction conversion. As reported in the literature [18], a layer of ZnO can be formed on a zinc surface under an O_2 atmosphere; furthermore, at temperatures above 370 °C, the rate of oxidation is related to the temperature and O_2 pressure by a complex parabolic rate law. It was, therefore, considered that the addition of NH_4NO_3 may not be necessary, as the protective ZnO layer can be generated if the Zn particles are suitably heated in the presence of oxygen.

For the preliminary trial, the zinc powder was pressed into a compacted cylinder with a packing density of ~3.4 g/cm^3 and was subsequently placed in a closed chamber, which had been used and described in detail in our previous study [15]. Next, the compacted powder was heated under an air atmosphere for 3 min using a nichrome coil with an electrical power of 300 W. The temperature vs. time history recorded by the thermocouples revealed that the surface temperature of the compacted powder increased to 370 °C in 20 s followed by a plateau showing a thermal steady state. After removing the heated sample from of the chamber, it was found to retain its shape and porosity. Moreover, the surface had turned a white color, probably due to the formation of the ZnO layer on the Zn particles. As the refractory ZnO skin would maintain the porous nature of the heated compacted powder, it was suggested that the heated sample could be ignited if a higher heating rate was applied because the oxygen supply would not be a problem. A considerable amount of Zn vapor may exist at elevated temperatures once sufficient heating power is supplied because of both the low melting and boiling point of Zn (b.p.$_{Zn}$ = 907 °C). Due to their differences in thermal expansion, the molten Zn and Zn vapor may crack the ZnO layer and flow out to be exposed to O_2, thereby providing an easier route for the oxidation of Zn. With this possibility in mind, two nichrome coils connected in parallel were used to increase the heating power. In this subsequent effort, the as-heated compact was ignited and completely combusted through the SHS using the increased heating power of up to 1000 W. A modified SHS method for synthesis of ZnO powder via a 2-step heating process was therefore developed.

2.2. Starting materials and synthesis process

The same zinc powder, used in the preliminary experiment described above, and a cylinder of oxygen gas (99.9% purity) were used as the starting materials. Six grams of Zn powder was placed in a stainless steel die with two plungers, and a compaction pressure of 20 MPa was applied to obtain a compacted cylinder of sufficient mechanical strength and porosity. The density of the compacted material was ~3.4 g/cm^3 with a 15 mm diameter and ~10 mm length.

Both the closed chamber, which contained a W-5% Re/W-25% Re thermocouple, and the configuration used for the temperature measurement have been shown schematically in our previous study [15]. The sample was placed on a height-adjustable stage in the closed chamber with the top surface 3 mm below the heating element and two nichrome coils connected in parallel. The variation in the temperature at the top of the sample was recorded using the thermocouple, which was held at a 20° angle relative to the surface of the compact and was pressed down with a small pressure to assure good contact. During the first heating step, the compacted powder was heated for 3 min after reaching thermal equilibrium at a surface temperature of approximately 370 °C using an electric current (300 W) passing through the nichrome coils. Next, the heating power was turned off, and the chamber was filled with oxygen at the desired gauge pressure (0–0.30 MPa). During the second heating step, 1000 W was applied to ignite the SHS reaction of the compacted powder. Once it was ignited, the electric power was turned off. The temperatures at which an abrupt temperature increase was observed and the maximum temperature during the SHS reaction were defined as the ignition temperature (T_{ig}) and the combustion temperature (T_c), respectively.

2.3. Product characterization

The as-obtained product was collected and removed from the reaction chamber for analysis after cooling to room temperature. The phase formed was identified by X-ray diffraction (XRD) using CuKα_1 radiation. The quantity of residual Zn in the product was determined via a gas evolution technique [15]. Approximately 100 ml of 15% $HCl_{(aq)}$ was added to 5 g of the as-obtained product, which had been ground thoroughly using an agate mortar and pestle. The quantity of the residual Zn was calculated from the volume of hydrogen gas evolved. The reaction conversion was defined as the weight ratio of Zn that had been converted to ZnO to that originally contained in the tested sample. For the as-obtained products that contained almost entirely zinc oxide, the $Zn^{2+}{}_{(aq)}$ concentration that was dissolved in the acidic solution was analyzed using an inductively coupled plasma-atomic emission spectrometer (ICP-AES) and compared to an external standard calibration curve, thereby determining the ratio of Zn to O. The morphology of the as-obtained product was observed by scanning electron microscopy (SEM). Photoluminescence (PL) spectra were measured at room temperature using a He–Cd laser with a wavelength of 325 nm as the excitation source.

The mZnOw–epoxy composites for microwave absorption measurements were prepared by gently mixing equally weighted samples of the as-obtained products with epoxy in a dispersion medium of ethyl acetate using a conditioning planetary mixer (Thinky ARE-250, Japan). The mixture was subsequently sprayed onto 150 mm × 150 mm aluminum plates and dried in oven at 100 °C for 10 min. When the surface of the composite coating had been dried, another layer was processed until the desired thickness of 1.5 mm was obtained. It was found that the morphology of the as-obtained products was preserved in the composite after the preparation procedure. For comparison, another composite sample containing ZnO particles with a grain size range of 20–50 nm was also prepared (the nano-sized ZnO particles were synthesized by the combustion reaction between zinc nitrate and glycine, as reported in our previous study [5]). To evaluate the sample's microwave-absorbing efficiency, the measurement of reflectivity (i.e., return loss) was conducted on the as-prepared composite backed with an aluminum plate using a Hewlett-Packard 8510 B vector network analyzer in the frequency range of 2–18 GHz.

3. Results and discussion

Figs. 1 and 2 show the SEM images and the corresponding XRD patterns of the different experimental stages as described in Section 2.1. The starting Zn powder consisted of spheres of ~2–10 μm in diameter (Fig. 1(a)). Before heating, the compacted reactant initially contained Zn only (Fig. 1(b)), and it was quenched as soon as its combustion reaction had been ignited in air. The quenched sample is porous and composed of agglomerated spherical particles and hollow, eggshell-like structures (Fig. 1(b)). Both the structures' size and shape are nearly identical to that of the starting Zn powder (see Fig. 1(a)). Judging by the XRD analysis, a small amount of ZnO was detected in the quenched sample (Fig. 2(b)). It is thought that the as-formed ZnO comes from the eggshell-like structures and the oxidized surface of the spherical particles. As shown in the XRD spectrum of the as-obtained product (Fig. 1(c)), the characteristic peaks of ZnO greatly increased, whereas those of Zn diminished. This finding indicated that a considerable amount of ZnO formed during the SHS reaction, but that some Zn remained in the as-obtained product. The microstructure of the as-obtained product consists of numerous multipod substances and a solidified melt (Fig. 2(c)), which represent the desired ZnO and unreacted Zn, respectively, as identified by energy dispersive spectrometry (EDS).

Fig. 3 shows the effects of the P_{O_2} on the ignition temperature, the combustion temperature, and the reaction conversion. The ignition temperature, ranging between ~750 and 950 °C, slightly decreases with increasing P_{O_2}. It is thought that the ignition of the SHS reaction may be associated with the substantial

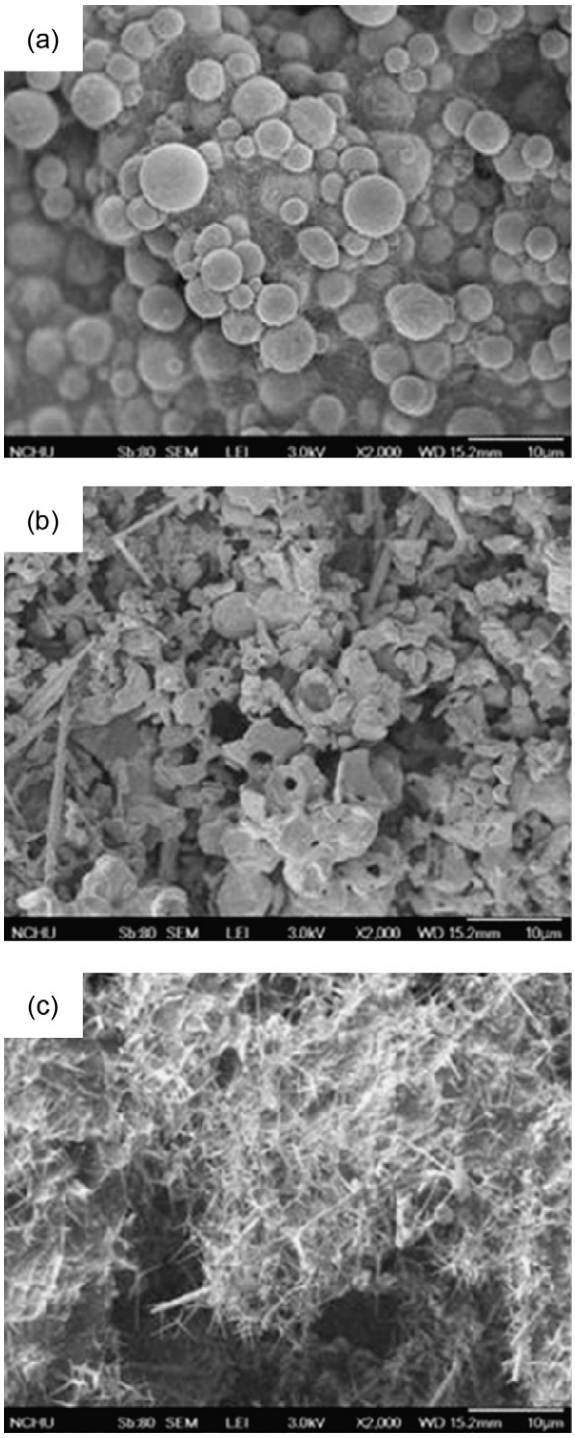

Fig. 1. SEM photographs of typical morphologies of (a) Zn powder used as the starting material in this study; (b) fractured surface of Zn-powder compact quenched just after being ignition, and (c) as-obtained product. (Note that the synthetic process was performed in air, i.e., the oxygen gauge pressure (P_{O_2}) = 0 MPa.)

formation of Zn vapor because the T_{ig}s are close to the boiling point of Zn. Evidence from the morphological observations supports this hypothesis. As shown in Fig. 1(b), the eggshell-like structures have a hollow, fractured appearance that may be caused by the Zn vapor escaping from the protecting layer. As both the temperature and the concentration of the Zn vapor increased to sufficient values for ignition, the SHS reaction occurred, and the temperature rose to the T_c. It is thought that the ZnO formed through the gas phase reaction between O_2 and Zn vapor at the elevated temperatures.

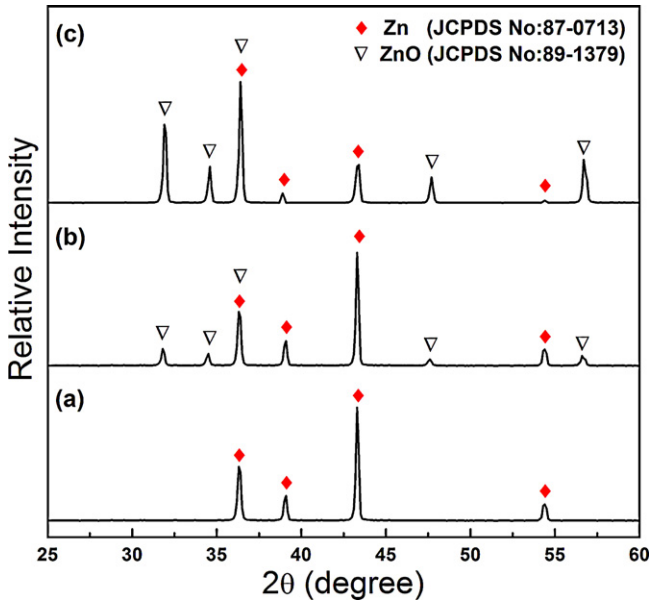

Fig. 2. XRD patterns of (a) Zn powder used as the starting material in this study; (b) fractured surface of Zn-powder compact quenched just after being ignition, and (c) as-obtained product. (The process was performed in air, i.e., P_{O_2} = 0 MPa.)

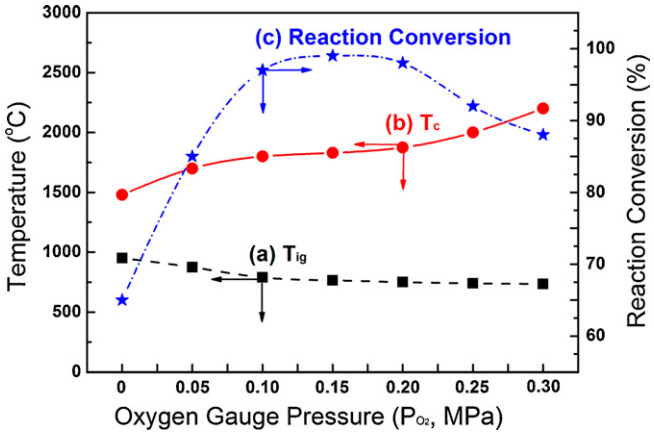

Fig. 3. Effects of P_{O_2} on (a) igniting temperature (T_{ig}), (b) combustion temperature (T_c), and (c) reaction conversion.

Subsequently, the nucleation and growth of ZnO led to the abundant formation of multipod whiskers (see Fig. 1(c)) via the mechanism of a multiple inversion-twin embryo [19]. The combustion temperature is within the range of ~1500–2200 °C and increases with increasing levels of P_{O_2}. The reaction conversion initially increases greatly with increasing P_{O_2}, up to ~98% from 0.10 to 0.20 MPa, and subsequently begins to decrease upon further increases. Based on experimental observations, the combustion front propagated more rapidly at increased P_{O_2}, due to the greater availability of oxygen inside the compacted reactant. This available oxygen may result in higher combustion temperature and reaction conversion as well. When a higher P_{O_2} was applied (≥0.3 MPa), however, a relatively rapid combustion explosively occurred almost simultaneously throughout the reaction volume. Under these conditions, the resulting combustion temperature was high enough to decompose and melt the ZnO (i.e., T_c > 1975 °C), giving rise to a decrease in the reaction conversion. Practically speaking, the heating element broke as the P_{O_2} was increased to 0.35 MPa due to the violent oxidation.

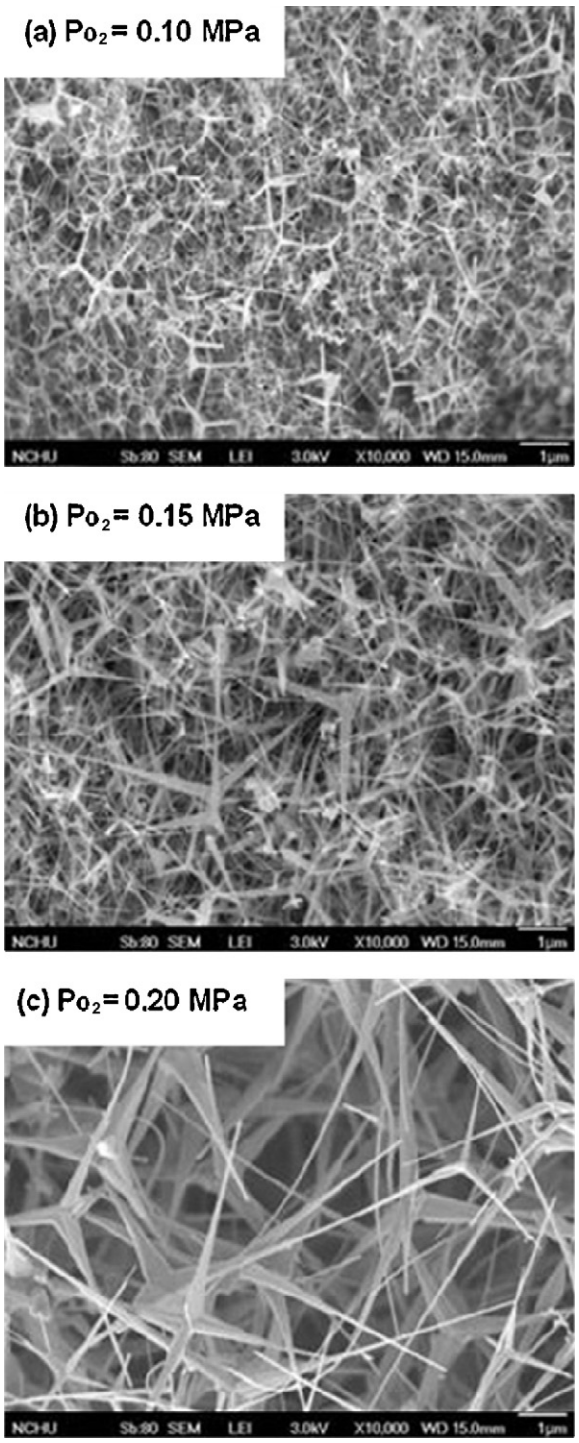

Fig. 4. Typical SEM images of as-obtained products synthesized at different P_{O_2}: (a) 0.10 MPa, (b) 0.15 MPa, and (c) 0.20 MPa.

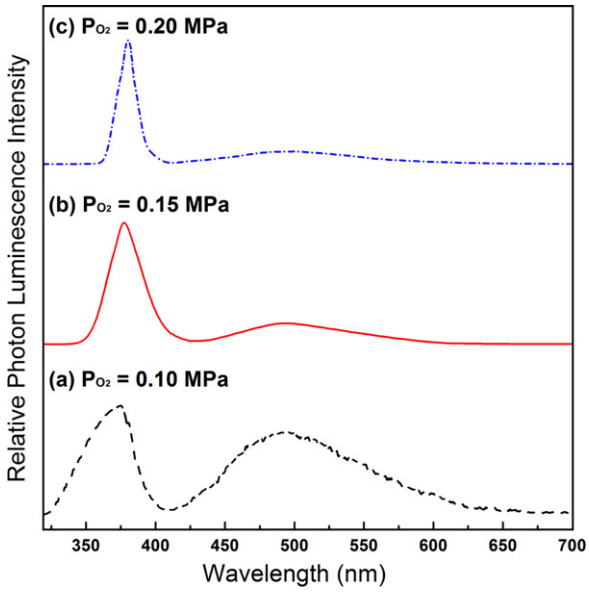

Fig. 5. Room-temperature photoluminescence (PL) spectra of as-obtained products synthesized at different P_{O_2}: (a) 0.10 MPa, (b) 0.15 MPa, and (c) 0.20 MPa.

In the following analyses, three representative products, which were synthesized at a P_{O_2} of 0.10, 0.15, or 0.20 MPa, were selected to study the effects of the P_{O_2} on the properties of the as-obtained products because of their nearly complete conversion. As shown in Fig. 4, the dimensions of the as-obtained mZnOw became larger when the P_{O_2} increased. This is a phenomenon that is ascribed to the higher T_c attainable with increasing oxygen pressure, thereby extending the time interval to allow a temperature that is high enough to favor the growth of mZnOw. The Zn:O atomic ratios are 1:0.862, 1:0.895, and 1:0.913 for the three products synthesized at a P_{O_2} of 0.10, 0.15, and 0.20 MPa, respectively. These results indicate that the products were nonstoichiometric and deficient in oxygen, which agrees with previously reported results regarding the preparation of mZnOw [11,14,20]. It was also found that the product had higher oxygen content when synthesized at a higher P_{O_2}, due to the greater amount of oxygen that is available to enters the ZnO crystal lattice and participates in the SHS reaction.

Fig. 5 shows the room-temperature PL spectra of the as-obtained products synthesized under different P_{O_2}. Each PL spectrum exhibited two significant emission peaks. One is a sharp, ultraviolet (UV) emission in the range of 375–380 nm corresponding to the near-band edge transition of a wide band gap, namely, the recombination of free excitons via an exciton-exciton collision process [3,11]; the other peak is a broad, green emission centered at ~500 nm, which is probably due to both the transition between a singly ionized oxygen vacancy (V_O^+) to a photoexcited hole [3,21] and the structure/surface defects [11,22]. The ratio in intensities of the intrinsic band gap of the UV emission and the defect-related green luminescence has been commonly used to evaluate the crystalline quality of ZnO [21,22]. It is thought that crystalline imperfections exist inside the as-obtained products because of the rapid changes in temperature and short reaction time inherent to the SHS method. It can be observed that this ratio tends to increase and that the UV emission peak becomes sharper as the P_{O_2} increases. This result, coupled with the results for the Zn-to-O composition ratio, implies that there is a reduction in the V_O^+ defects inside the ZnO crystal and an improvement in the crystalline quality. This finding is probably due to more oxygen entering the ZnO crystal lattice and the temperature required for crystallization being maintained for a longer duration. It is expected that the as-obtained product synthesized at $P_{O_2} = 0.20$ MPa may have a potential application as a UV-emitter.

Fig. 6 shows the reflectivity curves of the 1.5-mm thick composites containing the mZnOw synthesized at different P_{O_2} along with the nanocrystalline ZnO particle for comparison. As can be seen in this figure, the microwave-absorbing efficiency of the mZnOw–epoxy composite is superior to that of the composite containing ZnO particle. This result coincides with a similar study reported in Ref. [9] and may arise from the difference in shape between multipod- and particulate-ZnO. Compared to the ZnO particle, the three-dimensional, outwardly expanding structure of the

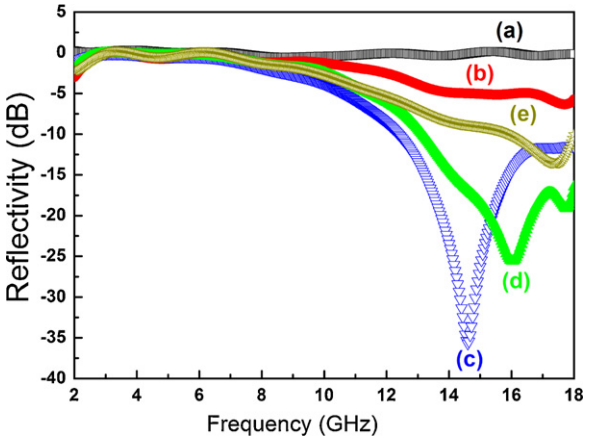

Fig. 6. Reflectivity curves for (a) epoxy resin, (b) composite of epoxy–50 wt% nanocrystalline ZnO particle, and composites of epoxy–50 wt% mZnOws synthesized at P_{O_2}: (c) 0.10 MPa, (d) 0.15 MPa, and (e) 0.20 MPa. (All of the tested samples were prepared with the same thickness of 1.5 mm.)

mZnOw not only has the advantage of forming continuous networks and tiny bubbles in the composite, but it can also act as charge-concentrating multipoles and quasi-antennae, due to its sharp tips and semiconductive branches, respectively [9,10]. These traits allow for certain actions, such as induced dissipative current, interfacial electric polarization [23], the dielectric confinement effect [24], and diffuse reflection of the incident microwave [25], which favor microwave absorption. As also shown in Fig. 6, all of the epoxy–mZnOw composites can attain a reflectivity <−10 dB in the range of 10–18 GHz; moreover, their absorption peak becomes stronger and broader with decreased P_{O_2}. The composite containing the mZnOw synthesized at a P_{O_2} of 0.10 MPa was found to possess the lowest reflection loss with −35 dB at ~14.8 GHz. It is thought that both the number of tips and pores in the composite increased simultaneously when a smaller-sized mZnOw, synthesized at a lower P_{O_2}, was used. This finding would favor the microwave-absorbing mechanisms as mentioned above. Our data reveal that the microwave-absorbing efficiency of the mZnOw–epoxy composite is comparable to that reported in the literature [9,10]. However, both additional experiments (such as measuring the relative permissivity, ε_r, and permeability, μ_r) and the theoretical derivation of reflectivity [26] are needed to make the mechanism clearer and to realize the potential of mZnOw for applications in microwave absorption that are currently being undertaken.

4. Conclusions

(1) An SHS method with green, economical, and practical advantages was developed to synthesize mZnOw via a 2-step heating approach using Zn powder as the starting material. A high reaction conversion (~98%) could be achieved under the P_{O_2} range of 0.10–0.20 MPa; moreover, both the size and Zn-to-O ratio of the as-obtained products were found to increase with the increasing P_{O_2}.

(2) Room-temperature PL measurements exhibited two emission peaks for the mZnOw products, the near band-gap UV emission located at ~378 nm and the broad defect related green emission centered at ~500 nm. The intensity ratio of these emissions increased with increasing P_{O_2}, which could be explained by the improved crystalline quality and reduced V_O^+ defects.

(3) It was verified that the microwave-absorbing efficiency of ZnO was significantly related to its dimensional size. Because the peculiar mZnOw structure causes certain mechanisms that favor microwave absorption, the efficiency of the mZnOw composites was superior to that of composites containing nanosized ZnO particles. Additionally, the efficiency of the mZnOw composites improved with the decreased size obtained at a lower P_{O_2}, which is most likely due to the presence of more pores, branches and tips in the composite.

Appendix A. Supplementary data

Supplementary data associated with this article can be found, in the online version, at doi:10.1016/j.jallcom.2011.09.033.

References

[1] Ü. Özgür, Y.I. Alivov, C. Liu, A. Teke, M.A. Reshchikov, S. Doğan, V. Avrutin, S.J. Cho, H. Morkoç, J. Appl. Phys. 98 (2005) 041301.
[2] S.J. Pearton, D.P. Norton, K. Ip, Y.W. Heo, T. Steiner, Prog. Mater. Sci. 50 (2005) 293.
[3] A.B. Djurišić, Y.H. Leung, Small 2 (2006) 944.
[4] S. Park, D.-W. Lee, J.-C. Lee, J. Am. Ceram. Soc. 86 (2003) 1508.
[5] C.-C. Hwang, T.-Y. Wu, Mater. Sci. Eng. B 111 (2004) 197.
[6] L.E. Greene, M. Law, J. Goldberger, F. Kim, J.C. Johnson, Y. Zhang, R.J. Saykally, P. Yang, Angew. Chem. Int. Ed. 42 (2003) 3031.
[7] P. Sagar, P.K. Shishoda, R.M. Mehra, H. Okada, A. Wakahara, A. Yoshida, J. Lumin. 126 (2007) 800.
[8] Y.-N. Zhao, M.-S. Cao, J.-G. Li, Y.-J. Chen, J. Mater. Sci. 41 (2006) 2243.
[9] Z. Zhou, L. Chu, S. Hu, Mater. Sci. Eng. B 126 (2006) 93.
[10] R.F. Zhuo, H.T. Chen, J.T. Chen, D. Yan, J.J. Feng, H.J. Li, B.S. Geng, S. Cheng, X.Y. Xu, P.X. Yan, J. Phys. Chem. C 112 (2008) 11767.
[11] N.-K. Park, G.B. Han, J.D. Lee, S.O. Ryu, T.J. Lee, W.C. Chang, C.H. Chang, et al., Curr. Appl. Phys. 6 (S1) (2006) e176.
[12] X. Sun, X. Chen, Y. Li, J. Cryst. Growth 244 (2002) 218.
[13] C.X. Xu, X.W. Sun, J. Cryst. Growth 277 (2005) 330.
[14] Q. Wan, K. Yu, T.H. Wang, C.L. Lin, Appl. Phys. Lett. 83 (2003) 2253.
[15] C.-C. Hwang, C.-S. Lin, G.-P. Wang, C.-H. Peng, S.-L. Chung, J. Alloys Compd. 467 (2009) 514.
[16] Z.A. Munir, Am. Ceram. Soc. Bull. 67 (1988) 342.
[17] C. Xu, W. Gao, Mater. Res. Innovations 3 (2000) 231.
[18] M.J. Tribelhorn, D.S. Venables, M.E. Brown, Thermochim. Acta 256 (1995) 309.
[19] Y. Dai, Y. Zhang, Z.L. Wang, Solid State Commun. 126 (2003) 629.
[20] T.K. Bhowmick, A.K. Suresh, S.G. Kane, A.C. Joshi, J.R. Bellare, J. Nanopart. Res. 11 (2009) 655.
[21] J. Zhou, Y. Wang, F. Zhao, Y. Wang, Y. Zhang, L. Yang, J. Lumin. 119–120 (2006) 248.
[22] A.B. Djurišić, W.C.H. Choy, V.A.L. Roy, Y.H. Leung, C.Y. Kwong, K.W. Cheah, T.K.G. Rao, W.K. Chan, H.F. Lui, C. Surya, Adv. Funct. Mater. 14 (2004) 856.
[23] Z. Zhou, L. Chu, W. Tang, L. Gu, J. Electrostat. 57 (2003) 347.
[24] Y. Chen, M. Cao, T. Wang, Q. Wan, Appl. Phys. Lett. 84 (17) (2004) 3367.
[25] M. Oku, Jpn. J. Appl. Phys. 32 (9b) (1993) 4377.
[26] Y. Michielssen, J.-M. Sager, S. Ranjithan, R. Mittra, IEEE Trans. Microwave Theory Tech. 41 (1993) 1024.